REVIEWED

Computer-assisted modeling and automatic controller adjustment for hydraulic drives based on an innovative nonparametric identification method

Marcus Helmke *, Simon Ströbel **, Prof. Dr.-Ing. Peter Anders** and Tobias Schulze ***

TRsystems GmbH, Automation, Eglishalde 16, 78647 Trossingen, Germany *
Furtwangen University, Tuttlingen Campus, Faculty of Industrial Engineering, Kronenstraße 16, 78532 Tuttlingen, Germany **
TU Dresden, Institute for Fluid Power, Chair of Fluid-Mechatronic Systems (Fluidtronics), Helmholtzstraße 7a, 01069 Dresden, Germany***
E-mail: marcus.helmke@trsystems.de, simon.stroebel@hs-furtwangen.de, peter.anders@hs-furtwangen.de, tobias.schulze2@tu-dresden.de

Model-based control and regulation concepts will become increasingly important due to their specific advantages, for example in respect of performance, stability, consideration of nonlinearities etc., for hydraulic drives in particular. The fundamental prerequisite for their application is sufficiently precise knowledge of the system's response characteristic. The prerequisite for their acceptance, however, is the availability of computer-supported tools, methods and algorithms, which enable a case-specific identification and controller design. This article presents a concept for achieving these goals on the basis of an innovative nonparametric identification method, which has proved to be extremely efficient in initial applications.

Keywords: hydraulic presses, characteristic diagram, operating point, model based control, self-learning control
Target audience: stationary hydraulics, industrial applications

1 Introduction

1.1 State of the art

Demands in terms of drawing cushion pressure control increasingly require a highly dynamic control behavior, which cannot be satisfactorily achieved using a classic PI controller based on control error (feedback controller) alone. Model-based approaches on the one hand and progress in the field of digital technology on the other have enabled new concepts in the control of hydraulic drives in recent years. Rather than generating the actuating signal exclusively via a feedback controller, the basic idea of these concepts is to additionally generate the signal via a process model calculated in real time in a precontrol circuit (feedforward controller). This is known as a two degrees of freedom control concept (2DOF control concept, see Fig. 1) which was first introduced by Horowitz /1/. Generally speaking: The higher the quality of the basic model, i.e. the better the model represents reality, the better the ultimately achievable control quality. In this concept the feedback controller essentially only has the task of compensating for inaccuracies in the precontrol model, but the main contribution to the overall actuating signal should be generated via the precontrol circuit. There are several approaches to design such a linear or nonlinear feedforward control. In /2/ the feedforward control algorithm for an injection moulding machine was based on the linear transfer function for example. In the field of drawing cushion pressure control, use of the nonlinear stationary drive characteristic diagram in the form of a nonparametric look-up table has proven itself time and again as a precontrol model /3/4/. Nonparametric means that no model equations are present, which must be parameterized through corresponding quantitative system parameters (surface areas, orifice coefficients, overlaps …). Instead, the look-up table only contains numerical values which, although they describe the static response characteristic with sufficient accuracy, no longer have any explicit functional correlation /5/. A purely theoretically derived characteristic diagram (white box characteristic diagram), which are essentially based on the datasheet values for the components used, are generally too inaccurate for the increased demands on control quality, which is why the actually existing drive characteristic diagram must be determined metrologically (black box characteristic diagram). Previous experiences show a connection between the effort involved in creating or identifying the real characteristic diagram and the quality of the feedforward control, i.e. the ultimately achievable control quality. The determination of a sufficiently accurate characteristic diagram is therefore generally associated with considerable measurement and commissioning effort. In particular, the execution of operating points in the limit ranges of drive systems frequently leads to difficulties.

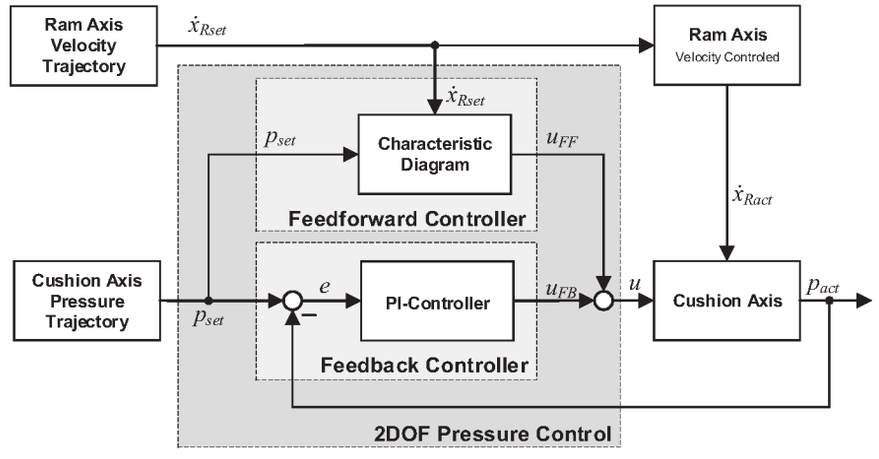

Figure 1: 2DOF structure for pressure control of cushion axis - state of the art

Use of the characteristic diagram-based feedforward control enables the actuating signal component of the PI controller in the sum actuating signal to be reduced to a fraction of 5%-10%, with a measuring scope of around 100 to 150 stationary points to be identified for determination of the characteristics. This not inconsiderable effort necessary for commissioning the feedforward control is also reflected on the maintenance side: Due to the wear on the flow edges of the valve, the system image generated during commissioning and the real flow behavior of the valve drift apart over time. At this point the maintenance engineer is forced to readjust the feedforward control with considerable measurement effort, which is why this adjustment is generally only performed after a valve replacement and poorer control characteristics are accepted in the meantime.

1.2 Motivation

The concept presented in this article presents an innovative method of identifying the drive characteristic diagram for the feedforward control, which uses both theoretical white box and metrologically obtained black box information. With even just a few stationary measuring points, however, this is able to deliver very good results during actuating signal generation, i.e. to represent the real characteristic diagram. As a result of the concept presented here, the commissioning and maintenance effort involved in hydraulic control should in principle be significantly reduced. The characteristics and results of the identification method are demonstrated using the example of the pressure control of a hydraulic try-out press of the type MW ZE2100 /6/. The identification method was performed offline, i.e. measuring data were recorded first of all and then the characteristic diagram identification was performed on the basis of the entire data material. When designing the identification method the fundamental requirement was set right from the beginning, however, that the process could in principle also be implemented in the form of online and real time-capable algorithms on a digital control computer, which can process the periodically occurring measuring data in the controller cycle, thus enabling an

adaptation/optimization of the precontrol model in virtually regular operation of the system. However, real-time implementation of the method has not been implemented yet.

A second concept for operating point-dependent adaptation of the feedback control parameters is also presented, which is again based on the (identified) drive characteristic diagram. Even if the feedback controller in the 2DOF concept no longer has the same fundamental importance as that of classic concepts for the reasons mentioned above, the feedback controller can now be parameterized to the precise operating point on the basis of the identified system model. Thus, in addition to the compensation of interference effects which cannot be acquired in the stationary characteristic diagram, corrections of the dynamic behavior can also be performed effectively and accurately. The entire 2DOF control design can therefore be considered as a coherent and logical overall concept. The design or parameterization of such a control no longer requires expert knowledge, but can also be algorithmized and automated. At present, however, this is still a theoretical concept, whose implementation and validation have not yet been performed on a real system.

2 Observed drive system

The concepts presented in the following for modeling the drive characteristic diagram for the feedforward control and the design of the feedback control parameters are derived and demonstrated using the specific example of a hydraulic 8-axis try-out press of the type MW ZE2100 /6/. This drive system will be described first of all and relevant model equations provided, which are necessary or helpful for the derivation and understanding of the methods described below. A single drawing cushion axis from the entire press is considered in the following.

2.1 System description

As shown in Figure 2, a drive axis essentially consists of a plunger and a highly dynamic (dual-flow) directional control valve of the type Moog D663 /7/, via which the discharged volume flow Q_V and consequently the relevant chamber pressure p can be regulated.

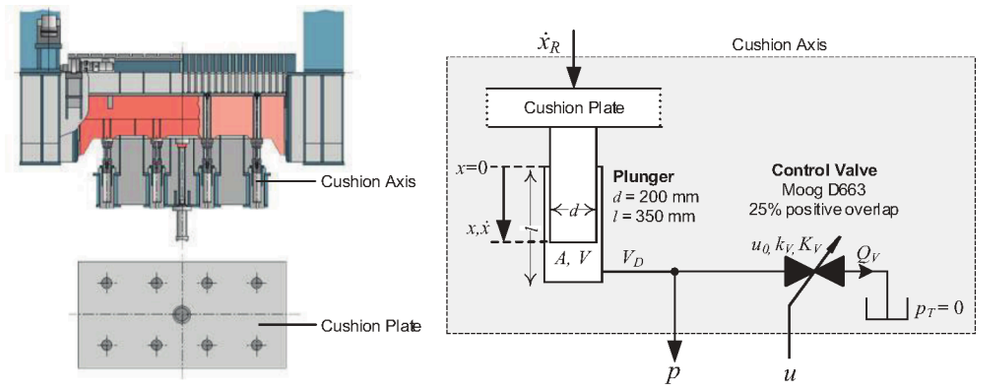

Figure 2: Drawing cushion drawing and technical diagram

The plunger with piston area A = 314cm² is externally impressed by the ram with speed $\dot{x}_R$ and it is always assumed in the following that $\dot{x}_R = \dot{x}$. The directional control valve is modeled as a simple discharge valve, whose degree of opening can be adjusted via the control voltage u = 0…+10V. The valve has a positive overlap of 25% (u_0 = +2.5V). Under the assumption of an ideal linear valve characteristic, the corresponding orifice coefficient follows from the datasheet values Q_{ref} = 350 l/min and p_{ref} = 5 bar, with k_V = 15.65 lpm/(V·bar$^{0.5}$). The movement impressed on the drawing cushion axis by the ram is an essential functional feature of drawing cushion drives. Only through the ram movement does a fluid compression and thus a pressure build-up in the chamber take place. From the point of view of the pressure control to be executed via the discharge valve, however, this impressed movement or the corresponding kinematic volume flow $Q_{kin} = \dot{x} \cdot A$ should be understood as the essential disturbance variable, which must be compensated almost constantly in order to maintain the required pressure p_{set}.

2.2 Model equations

The following four essential model equations can be specified for the volume flows Q_V (volume flow discharged via the valve → orifice equation) and Q_{kin} (kinematic volume flow), the chamber pressure p and the chamber volume V:

$$Q_V = \begin{cases} k_V \cdot u \cdot \sqrt{p} & for \quad u_0 \le u \le 1 \\ 0 & 0 \le u \le u_0 \end{cases} \qquad Q_{kin} = A \cdot \dot{x} = A \cdot \dot{x}_R \tag{1}$$

$$\dot{p} = \frac{1}{C_H(x)} \cdot Q_{comp} = \frac{E_{Fl}}{V(x)} \cdot (Q_{kin} - Q_V) \qquad V(x) = A \cdot (l - x) + V_{dead} \tag{2}$$

The valve dynamics is at first deliberately ignored at this point. The influence of the valve dynamics is discussed in section 4 in the design of the feedback control parameters.

3 Modeling, identification and optimization of the drive characteristic diagram

3.1 Definition of operating point and characteristic diagram

All stationary operating points accessible from a drive axis are ideally mapped in the drive characteristic diagram. An operating point **OP** is defined as the triple of a power flow variable (here speed $\dot{x}$), a power potential variable (here chamber pressure p) and the actuating variable (here valve voltage u). A specific operating point can be seen as an individual element of the characteristic diagram **CD**. The flow variable is usually applied in the characteristic diagram depending on the potential and actuating variable. Therefore $\dot{x}$ can here be formally regarded as on output variable dependent on the input variables p and u, where $\mathbf{x} = (p,u)^T$ describes the so-called input vector in the following. In summary, it can be stated that:

$$\mathbf{OP} = (p, u, \dot{x}) \qquad \mathbf{OP} \in \mathbf{CD} \qquad \dot{x} = f(\mathbf{x}) \tag{3}$$

Comment: It should be noted that $\dot{x} = f(\mathbf{x}) = f(p,u)$ is a purely formal and, for the following relationships, advantageous representation of the facts. From the viewpoint of the drawing cushion axis or the control task in accordance with Figure 1, the ram speed $\dot{x}_R = \dot{x}$ forms an input variable (disturbance variable) and the chamber pressure p forms the output variable (target variable) of interest in the controlled system.

3.2 White box characteristic diagram – Theoretical modeling

A theoretical white box characteristic diagram can be calculated for any drive system on the basis of corresponding model equations. As the characteristic diagram is a stationary model, dynamic effects (state changes) can and must be ignored in the model equations, therefore $\dot{p} = 0$ applies in the present case. In concrete terms this means that compression volume flows are ignored in the stationary observation. This is often a valid assumption, however, if the kinematic volume flows are dominant in relation to the compression volume flows in the relevant application. Under the assumption $Q_V = Q_{kin}$, the speed $\dot{x}$ depending on the pressure p and the actuating variable u results in the following, without further derivation:

$$\dot{x}_W(p,u) = \begin{cases} \frac{k_V}{A} \cdot u \cdot \sqrt{p} & for \quad u_0 \le u \le 1 \\ 0 & 0 \le u \le u_0 \end{cases} \tag{4}$$

The additional index W indicates that this is a theoretical *white box* description. This is a *parametric* (→ formula-based) representation of the characteristic diagram. If the p-u input space is suitably rasterized, for each of the possible p-u input variable combinations the relevant speed value can be explicitly calculated and stored in the form of a two-dimensional *nonparametric* look-up table with m rows and n columns.

CD	$u_1 = u_{\min}$	u_2	$\cdots$	$u_n = u_{\max}$
$p_1 = p_{\min}$	$\dot{x}_{11}$	$\dot{x}_{12}$	$\cdots$	$\dot{x}_{1n}$
p_2	$\dot{x}_{21}$	$\dot{x}_{22}$	$\cdots$	$\dot{x}_{2n}$
p_3	$\dot{x}_{31}$	$\dot{x}_{32}$	$\cdots$	$\dot{x}_{3n}$
$\vdots$	$\vdots$	$\vdots$	$\ddots$	$\vdots$
$p_m = p_{\max}$	$\dot{x}_{m1}$	$\dot{x}_{m2}$	$\cdots$	$\dot{x}_{mn}$

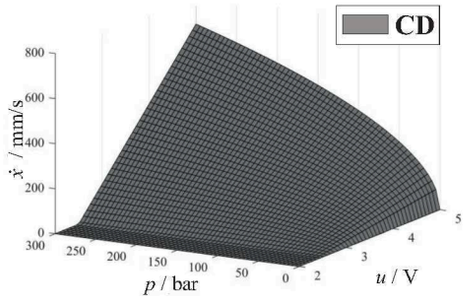

Figure 3: Look-Up Table and White Box Characteristic Diagram

From this look-up table, through specification of the set points p_{set} and $\dot{x}_{Rset}$ the actuating variable u_{FF} of the precontrol circuit can basically be calculated using suitable algorithms, e.g. bilinear interpolation, in accordance with Figure 1:

$$u_{FF} = f(p_{set}, \dot{x}_{Rset}) \tag{5}$$

Comment: The actuating signal component which is necessary in a defined load situation for compensation of the (expected) kinematic volume flow $Q_{kin} = \dot{x}_{Rset} \cdot A$, is therefore calculated de facto via the characteristic diagram. The characteristic diagram-based feedforward control can thus be seen quasi as a load-dependent disturbance variable compensation. Compression volume flows, which are required for a change in the pressure of the fluid (→ dynamic process), are ignored by this stationary model as a matter of principle. These model errors must therefore be compensated by the feedback controller in a 2DOF control concept.

3.3 Black box characteristic diagram – measurement-based identification

The theoretical white box characteristic diagram inevitably contains a multitude of inaccuracies or errors. Possible causes can, for example, be a non-ideal linear valve characteristic, effects not taken into account in the model (e.g. friction/leakage), non-ideal model assumptions (e.g. no ideal root-shaped relationship between volume flow and pressure) or deviations from the datasheet values due to manufacturing tolerances and wear. In the specific case of the MW ZE2100 deep drawing press, valves with a special piston were also used which, although they have a volume flow signal function that is advantageous for the application, differ considerably from the relevant datasheet value in terms of quantity. In this case the white box characteristic diagram is so flawed, that it is de facto unusable for the precontrol circuit.

Due to the resulting inadequate quality of the white box model, a measurement-based identification of the real characteristic diagram of each individual axis is generally performed instead. Previously this identification took the form of a classic point-for-point identification. That is, the largest possible number N of stationary operating points are approached and the identified operating points $\mathbf{OP}_B = (p_B, u_B, \dot{x}_B)$ are stored in a look-up table, similarly to the white box characteristic diagram. Index B stands here for observation/measurement = *black box* Information. The advantage of this approach is that the resulting characteristic diagram maps the real response characteristic of the drive system quasi optimally. The use of a nonparametric look-up table for mapping the static response characteristic has the fundamental advantage, in comparison to any parametric (equation-based) approach, that each data value in the table represents virtually any chosen degree of freedom. On the one hand no system parameters have to be determined from the measured data (no parameter fitting or similar identification methods necessary), and on the other hand it is irrelevant whether corresponding effects have been mapped incorrectly or not at all in the white box model equations: In the observed response characteristic in the form of an actually measured operating point $\mathbf{OP}_B$, all technical and physical effects which lead to the observed combination of power flow, power potential and actuating variable at this operating point are cumulatively mapped. For a control it is irrelevant why this particular combination is present at the observed operating point; a control only has to generate the correct actuating signal for the respective operating point. The disadvantage is, on the one hand, that this method is very time-consuming, as previously mentioned, since the largest possible number of operating points ($N \approx$ 100-150) should be approached, as part of the real characteristic diagram, for an accurate identification. On the other hand, however, many relevant operating points cannot even be approached, as due to the system dynamics in real operation and the limited cylinder stroke in limit ranges, no secured stationary state can be adopted and the measured data cannot, or rather may not, be interpreted as part of the real characteristic diagram.

3.4 Gray box characteristic diagram – measurement-based optimization

An innovative method for determining the real characteristic diagram is described in the following, which effectively combines the advantage of white box modeling (quickly accessible) and black box identification (highly precise) into a so-called gray box model. It is assumed that the white box characteristic diagram represents a qualitatively plausible description of the stationary response characteristic, even if this is not quantitatively correct on account of the modeling errors. This qualitatively approximately correct model will be corrected by a few ($N \approx$ 10-15 or even less) additional black box observations, as a result of which the measurement and commissioning effort can be reduced to around 10% of the original value. This is therefore not a classic measurement-based identification method, but can rather be seen as a measurement-based *optimization* method. This method basically comprises two steps: First, all transient system states must be reliably separated out from the accumulated measured data, so that reliable measured black box operating points, which can effectively be interpreted as unique "fingerprints" of the real characteristic diagram area, can be specified as a result. To this end a method based on time-discrete filter algorithms was developed, which will not be explained in more detail here, however. For all such operating points reliably identified as stationary, the error between the black box observation and the white box model must then be determined in a second step. If this error is related to the original white box data value, a corresponding relative/percentage error can be specified at the respective operating point defined through the input variable combination $\mathbf{x}_B = (p_B, u_B)$:

$$e_{rel}(\mathbf{x}_B) = \frac{\dot{x}_B(\mathbf{x}_B) - \dot{x}_W(\mathbf{x}_B)}{\dot{x}_W(\mathbf{x}_B)} \tag{6}$$

As only a few selected operating points $\mathbf{OP}_B = (p_B, u_B, \dot{x}_B)$ will be specifically identified in principle, the measurement-based information relating to the model errors must be suitably *generalized* for the entire characteristic diagram area, i.e. across the entire input space $\mathbf{x}$. Assuming this is possible, a gray box data value can be calculated at *each* point $\mathbf{x}$ of the input space (i.e. not only at the specifically observed points $\mathbf{x}_B$) in accordance with the following rule:

$$\underbrace{\dot{x}_G(\mathbf{x})}_{Gray\ Box} = \underbrace{\dot{x}_W(\mathbf{x})}_{White\ Box} \cdot \underbrace{\left(1 + e_{rel}(\mathbf{x})\right)}_{Black\ Box} \tag{7}$$

In short, this means that each original white box data value adapts on the basis of the relative model error determined at this point, i.e. the look-up table numerical value is increased or decreased accordingly. The question is therefore how the few relative model errors explicitly known at the points $\mathbf{x}_B$ can be generalized. It is plausible to assume here that in the local environment of a specifically identified operating point the relative model error is likely to be of a similar quantity to that at the identified operating point itself. However, as you move further away from this reliably identified point in the input space, this assumption becomes increasingly unreliable, or rather, more improbable. The model errors must therefore be meaningfully interpolated between the explicitly known points. A Normalized Radial Basis Function Network (NRBF), a special class of Artificial Neural Networks (ANN), is used for this purpose (see e.g. /8/ for further theoretical explanations and derivations). Each individual identified operating point $\mathbf{OP}_B$ effectively forms a neuron of this network, where $\mathbf{x}_B$ forms the basis of the respective neuron (= position in input space) and $e_{rel}(\mathbf{x}_B)$ the so-called neuron weight. The model errors at each point of the input space are calculated in accordance with the NRBF interpolation rule:

$$e_{rel}(\mathbf{x}) = \frac{\sum_{B=1}^{N} e_{rel}(\mathbf{x}_B) \cdot \psi_B(\mathbf{x})}{\sum_{B=1}^{N} \psi_B(\mathbf{x})} \tag{8}$$

With basic function ψ and distance d:

$$\psi_B(\mathbf{x}) = \exp\left(\frac{d(\mathbf{x})^2}{2\sigma_B^2}\right) \qquad d(\mathbf{x}) = \|\mathbf{x} - \mathbf{x}_B\| = \sqrt{(\mathbf{x} - \mathbf{x}_B)^T \cdot (\mathbf{x} - \mathbf{x}_B)} \tag{9}$$

The parameter σ_B is the so-called form or expansion parameter of a neuron, which expresses the expansion of an individual neuron and thus the degree of overlap of all neurons. This must be defined using suitable algorithms for each neuron, based on the number and distribution of all existing neurons. In the present case this parameter tells us, put simply, how far an identified operating point $\mathbf{OP}_B$ may disseminate the information relating to "its" model error $e_{rel}(\mathbf{x}_B)$ in the input space and thus influence/correct other points $\mathbf{x}$. Figure 4 illustrates the NRBF structure as a block diagram according to equation (8).

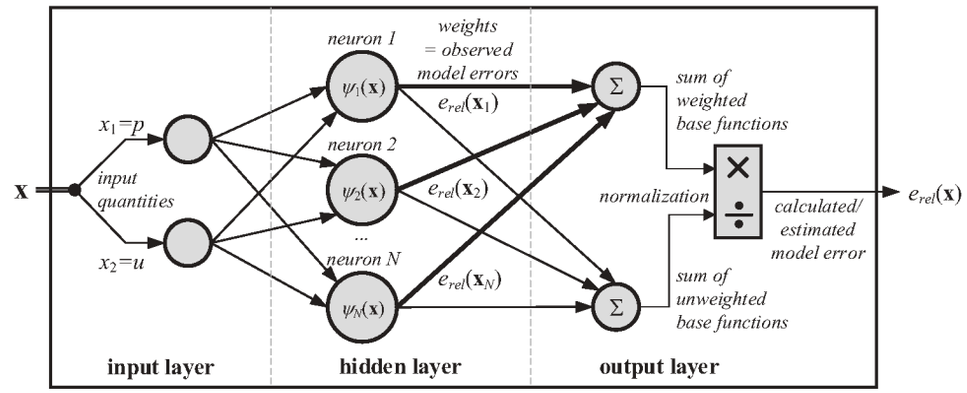

Figure 4: NRBF structure

On the observed deep drawing press, $N = 10$ example operating points were approached, identified as stationary black box operating points and used for the characteristic diagram optimization. The resulting NRBF network consequently has N =10 neurons. Figure 5 shows the original white box model $\mathbf{CD}_W$, the black box database $\mathbf{OP}_B$ and the resulting gray box characteristic diagram $\mathbf{CD}_G$. On the one hand the specifically identified operating points are clearly very well "matched" by the gray box characteristic diagram, and on the other hand the relevant information is meaningfully generalized for the entire input space.

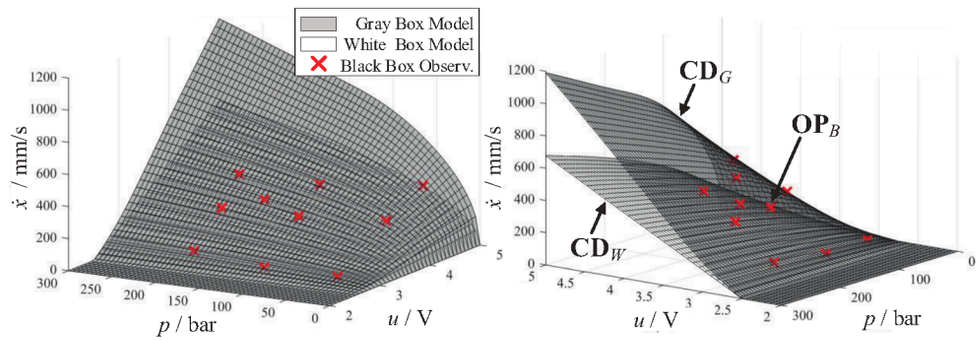

Figure 5: White Box and Black Box Characteristic Diagram

3.5 Control results with black box and gray box characteristic diagram

Comparison measurements were performed on the real deep drawing press, where on the one hand the originally implemented black box characteristic diagram and on the other hand the gray box characteristic diagram determined with the new NRBF optimization method were used as the precontrol model in the 2DOF control concept, and the PI feedback controller was also identically parameterized in all tests. The results of one of the eight axes of the deep drawing press are shown in Figure 6, where a) shows the results with reference variable step change and b) shows the results with disturbance variable step change.

It was expected that the control results would be virtually identical in the ideal case, with the advantage of the gray box characteristic diagram consisting almost exclusively in a reduced identification effort. It was observed, however, that with the gray box characteristic diagram even slightly better results could be achieved in the static and dynamic control behavior than previously. This could be due to the fact that the valve wear occurring since the original black box identification is reflected better in the more recent data used for the gray box characteristic diagram. In any case, however, it can be said that the gray box characteristic diagram generated through the NRBF interpolation can be achieved even with only a very approximately correct white box model as the starting point, and that a very good mapping of the real static response characteristic can be achieved based on a small number of measured data. Any nonlinearities implicitly present in the measured data, which were not included in the original white box model, are also recorded and mapped.

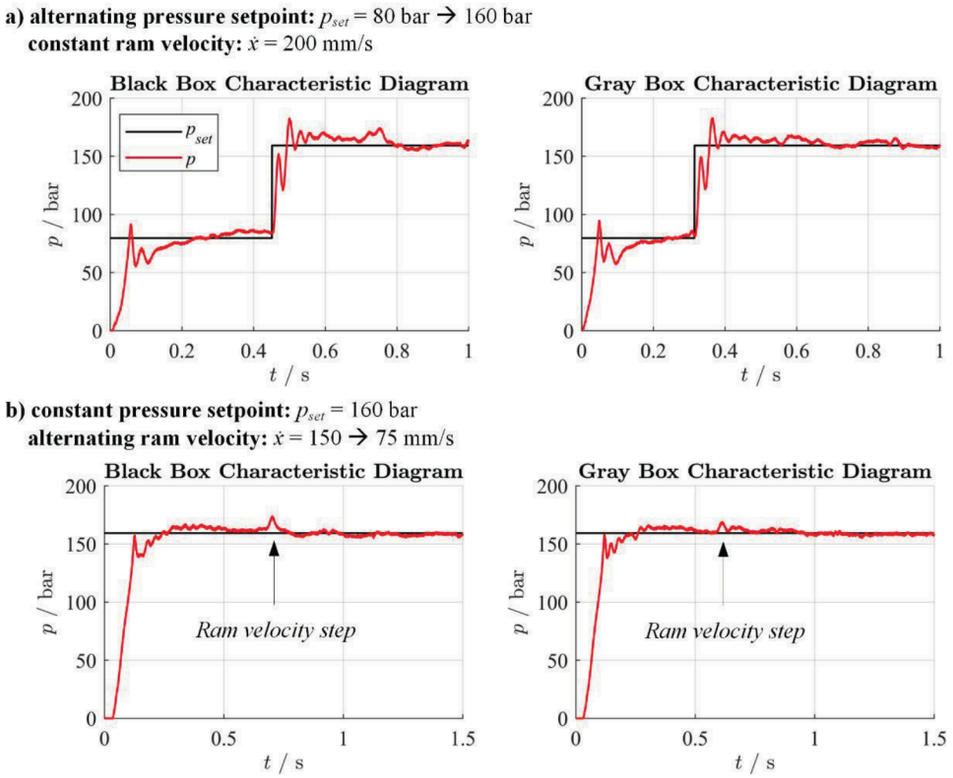

Figure 6: Control Quality with Black Box and White Box Characteristic Diagram

4 Operating point-dependent adaptation of the feedback control parameters

For the complete design of a control according to the 2-DOF concept, in addition to the feedforward control the classic feedback controller (PI controller) must also be parameterized, even if this no longer has the dominant role in the overall concept with a precisely tailored feedforward control. However, if one of the great advantages of the 2-DOF concept should be that the dominant nonlinearities of the system can also be taken into account via the precontrol circuit, then with distinctly nonlinear systems like hydraulic drives, the design of the feedback controller according to the classic methods of linear control theory (see /9/ for example) represents a certain

fracture within the overall concept, as the system must be linearized at a selected operating point. The consequence is that the feedback controller must either be designed based on the worst-case operating point and sub-optimal solutions must therefore be accepted at other operating points, or that the parameters of the controller must be adapted in real time operating point-dependently. In this last section we will show, using the example of the deep drawing press, that with in-depth knowledge of the response characteristic of the control system, which must in any case be available in model-based controls, the control parameters can also be adapted operating point-dependently in real time.

4.1 General observations

As explained above, the actuating signal component of the precontrol circuit ensures the provision of a volume flow component, which ideally largely compensates for the pressure-changing effect of the kinematic volume flow completely and in real terms. However, if this actuating signal component is generated without the involvement of the feedback controller, the following situation results:

1. From its perspective the piston is stationary, as the feedback controller obviously does not have to provide/compensate for any kinematic volume flow.
2. The pressure adapts to the set course "miraculously by itself", thanks to the feedforward control.
3. The hydraulic capacity nevertheless changes over the time $C_H = C_H(t)$

4.2 Nonlinear pressure build-up equation

For a further mathematical analysis the differential equation specified at the outset for the pressure build-up is considered:

$$\dot{p} = \frac{E_{Fl}}{V(x)} \cdot (Q_{kin} - Q_V) \quad \xrightarrow{yields} \quad \underbrace{\frac{V(x)}{E_{Fl}} \cdot \dot{p}}_{\text{Term 1}} = \underbrace{A \cdot \dot{x}}_{\text{Term 2}} - \underbrace{k_V \cdot u \cdot \sqrt{p}}_{\text{Term 3}} \tag{10}$$

This is a first order differential equation, where two of the three occurring terms, terms 1 and 3 are nonlinear. A linear model of the control system - i.e. of the pressure build-up in the chamber in this case - is required as the basis for the design of the feedback controller. This occurs in principle by linearizing the above pressure build-up equation. The following facts can be recorded first of all:

1. The prefactor $V(x)/E_{Fl}$ of the first term relates to the hydraulic capacity of the chamber. This should represent a constant for the respective linearization range. If we assume, as is customary and acceptable in a first approximation when designing a linear controller, that the effective bulk modulus E_{Fl} is constant, then on account of $V(x)$ the prefactor must normally be permanently adapted stroke-dependently.
2. The second term relates to the kinematic volume flow, which is ideally completely provided or compensated for via the feedforward control. As mentioned above, this can be interpreted from the perspective of the feedback controller as meaning that the piston is stationary and $\dot{x} = 0$ can therefore be assumed in the following, as a result of which the entire term can be omitted for further considerations.
3. The third term relates to the flow equation for the valve $Q_V(p,u)$ with a dual nonlinearity: The root function itself represents one and the product of the time-varying root function as a signal with another time-varying signal represents the other nonlinearity. The linearization of this relationship must occur at a suitable stationary operating point **OP**. The respective current operating point must be used as such for logical reasons. This is therefore defined by the current actuating variable u for the kinematic volume flow and the current chamber pressure p.

4.3 Linearized pressure build-up equation

The linearization of the flow relationship Q_V (Term 2) at an operating point **OP** = (p_{OP},u_{OP}) (defined by the kinematic volume flow!) follows mathematically according to:

$$\hat{Q}_V = \underbrace{\left(\frac{\partial Q_V}{\partial p}\Big|_{\mathbf{OP}}\right)}_{K_p} \cdot \hat{p} + \underbrace{\left(\frac{\partial Q_V}{\partial u}\Big|_{\mathbf{OP}}\right)}_{K_u} \cdot \hat{u} \tag{11}$$

With the two resulting linearization factors

$$K_p = \frac{k_V \cdot u_{\mathbf{OP}}}{2 \cdot \sqrt{p_{\mathbf{OP}}}} \qquad K_u = k_V \cdot \sqrt{p_{\mathbf{OP}}} \tag{12}$$

The pressure build-up equation at the operating point is therefore, in deviation variables (indicated by the additional hat above variables)

$$\frac{V(x)}{E_{Fl}} \cdot \dot{\hat{p}} = -\left(K_p \cdot \hat{p} + K_u \cdot \hat{u}\right) \quad \xrightarrow{yields} \quad \frac{V(x)}{E_{Fl} \cdot K_u} \cdot \dot{\hat{p}} + \hat{p} = -\frac{K_p}{K_u} \cdot \hat{u} \tag{13}$$

Or with the substitutions

$$T_S = \frac{V(x)}{E_{Fl} \cdot K_p} \qquad K_S = -\frac{K_u}{K_p} \tag{14}$$

the differential equation follows:

$$T_S \cdot \dot{\hat{p}} + \hat{p} = K_S \cdot \hat{u} \tag{15}$$

This is the linear differential equation of the pressure build-up in the chamber for the speed-compensated case. The control must reduce the valve opening degree at a given kinematic volume flow in order to increase the pressure, and vice versa. This intuitively obvious fact is expressed in the differential equation in the sign reversal in the coefficient K_S of the excitation term on the right-hand side of the differential equation. With (15) a first order differential equation is now available, which describes the dynamic behavior of the control system, at least as long as the operating point is sufficiently close to the operating point defined by dead volume, kinematic volume flow and chamber pressure.

The following fact is important for the considerations below: Both parameters of the control system T_S and K_S are dependent on the linearization parameters K_p and K_u. These were determined by linearization of the parametric white box model equation at a *stationary operating point* **OP**. However, the linearization parameters are de facto nothing more than the gradients (dQ/dp and dQ/du) of the *stationary characteristic diagram* at that operating point. The numerical determination of the gradients from a numerical look-up table is almost trivial, however, and can easily be performed in real time. The current gradients or linearization parameters can thus also be determined from the gray box characteristic diagram, which reflects reality very well, in any controller cycle, and be assumed as known for further considerations.

4.4 Design of the feedback control parameters

The transfer function of the control system follows from (15):

$$G_S(s) = \frac{p(s)}{u(s)} = \frac{K_S}{T_S \cdot s + 1} \tag{16}$$

A PI controller can be used to control such a PT_1 system: This is permissible and sensible in system theory terms on the one hand, as the present case relates to a system with self-regulation and therefore in principle an integral controller component is necessary for the complete compensation of control errors that remain stationary. On the other hand it is dynamically sensible, as the respective operating point is mostly impressed by the feedforward

control in principle, and does not have to be assumed through large-scale integration of the integral controller branch. With the transfer function of a PI controller

$$G_R(s) = K_R \cdot \frac{T_{ZR} \cdot s + 1}{s} \tag{17}$$

it therefore follows for the open control loop

$$G_{OL}(s) = G_R(s) \cdot G_S(s) = \left(K_R \cdot \frac{T_{ZR} \cdot s + 1}{s}\right) \cdot \left(\frac{K_S}{T_S \cdot s + 1}\right) \tag{18}$$

The zero point (time constant) T_{ZR} of the controller is freely selectable in principle. If in accordance with

$$\boxed{T_{ZR} = T_S = \frac{V(x)}{E_{Fl} \cdot K_p}} \tag{19}$$

this is selected as being equal to the system time constant T_S, in order to compensate the latter, these formally cancel each other out in the open control loop:

$$G_{OL}(s) = \frac{K_R \cdot K_S}{s} \tag{20}$$

After closing the control loop, the controlled pressure chamber (again) has a PT_1 structure:

$$G_{CL}(s) = \frac{G_{OL}(s)}{1 + G_{OL}(s)} = \frac{\frac{K_R \cdot K_S}{s}}{1 + \frac{K_R \cdot K_S}{s}} = \frac{1}{\left(\frac{1}{K_R \cdot K_S}\right) \cdot s + 1} = \frac{1}{T_{CL} \cdot s + 1} \tag{21}$$

The time constant $T_{CL} = 1/(K_R \cdot K_S)$ can *theoretically* be arbitrarily small and the system can thus be made arbitrarily "sharp". This is possible in real terms but only provided that no significant limitations occur in the real system, which limit this dynamic behavior. This would be the case e.g. if a step response were required to a unit step of the control signal u via the time constant of the control loop, which the system cannot provide because the valve cannot supply the necessary volume flow quantity. Even if the value K_S (from the characteristic diagram) can be assumed as known, the question remains of how great a controller gain K_R can then be selected, through which the time constant T_{CL} is ultimately defined:

$$K_R = \frac{1}{T_{CL} \cdot K_S} = -\frac{K_p}{T_{CL} \cdot K_u} \tag{22}$$

Within the framework of the linear theory any PT_1 system can be made arbitrarily fast, and first-order systems cannot become unstable as long as no gradient reversal (→ change of sign of a parameter of the transfer function) occurs. The limit is therefore predefined by reality-based limitations alone. Such a limit should, however, always exist if the valve dynamics were not taken into account in the previous considerations, i.e. it has been assumed that the valve is infinitely fast and can therefore make the transition to a new operating point within an infinitely short time. This is of course not the case in reality. The dynamics of the pressure change are therefore, in the present case, predefined solely by the fastest possible volume flow change which the existing valve can provide. A dynamic limitation, as results in other systems, for example, due to the maximum possible pump rotation speed, is not present here. However, the build-up of the volume flow in the valve requires a certain time, which is for example described operating point-dependently via the valve time constant T_V (rate of rise $\dot{Q}_V = dQ_V/dt$ of the volume flow step response of the valve) and can generally be taken or estimated from the valve datasheet (Figure 7 a) /7/).

The time constant T_V of the actuator should be faster by a factor k (usually e.g. $k = 10$) than the time constant T_S of the controlled system. The time constant $T_{CL} = k \cdot T_V$ of the controlled system must therefore be selected depending on the valve dynamics. From this, the required controller gain follows:

$$\boxed{K_R = \frac{1}{T_{CL} \cdot K_S} = -\frac{K_p}{(k \cdot T_V) \cdot K_u}} \tag{23}$$

In summary it can be stated that both PI control parameters T_{ZR} and K_R can be designed/adapted meaningfully or optimally with the help of the (measured) piston position x (→ current hydraulic capacity) and the characteristic diagram gradients $K_p = dQ/dp$ and $K_u = dQ/du$ (linearization parameters). The dynamics of the closed control loop are ultimately only limited by the dynamics of the actuator, i.e. the valve (valve time constant T_V):

$$\boxed{T_{ZR}(K_p, x) = \frac{V(x)}{E_{Fl} \cdot K_p}} \qquad \boxed{K_R(K_p, K_u) = -\frac{K_p}{k \cdot T_V \cdot K_u}} \tag{24}$$

a) Estimation of valve timeconstant

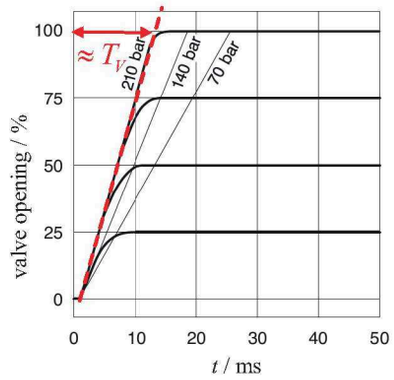

b) Calculation of linearization parameters / gradients

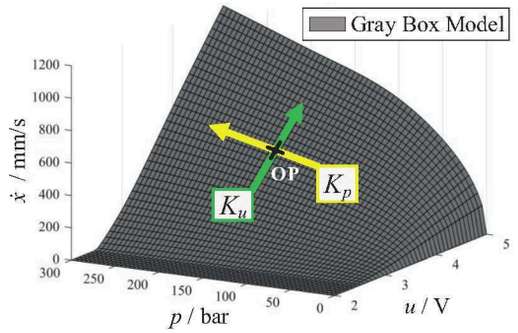

Figure 7: Determination of the feedback control parameters

4.5 Outlook: Model-based compensation of compression volume flows

The volume flows in a hydraulic system can in principle be divided into kinematic volume flows, i.e. the volume flows necessary for movement, and compression volume flows, for changing the pressure in the chamber. As mentioned above, the characteristic diagram-based feedforward control ideally applies exactly the actuating signal necessary for compensation of the kinematic volume flow. This is interpolated from the look-up table according to (5):

$$u_{FF}^{kin} = f(p_{set}, \dot{x}_{set}) \tag{25}$$

The feedback controller must consequently compensate for the (remaining) model error in the feedforward control on the one hand, and on the other hand generate the actuating signal necessary for the compression volume flows. If we think the entire model-based situation through logically to the end, however, the provision of an actuating signal component necessary for the compression volume flows is also possible in principle using a model-based approach, with a further parallel precontrol circuit. The linearized differential equation for the pressure build-up is considered again for this purpose:

$$T_S \cdot \dot{\hat{p}} + \hat{p} = K_S \cdot \hat{u} \tag{26}$$

If we assume that the current pressure p_{OP} corresponds to the current setpoint value p_{set} (current control goal reached, control error $e = 0$) and there is no pressure change at the current operating point $\dot{p}_{OP} = 0$ (assumption of a stationary state), then this follows for the deviation variables resulting from the linearization:

$$\hat{p}_{set} = p_{set} - p_{OP} = 0 \tag{27}$$

$$\dot{\hat{p}}_{set} = \dot{p}_{set} - \dot{p}_{OP} = \dot{p}_{set} - 0 = \dot{p}_{set} \tag{28}$$

The differential equation is thus simplified as follows

$$T_S \cdot \dot{p}_{set} = K_S \cdot \hat{u} \tag{29}$$

By releasing the actuating variable we then get:

$$u_{FF}^{comp} = \frac{T_S}{K_S} \cdot \dot{p}_{set} \tag{30}$$

This actuating signal component is exactly the component that is necessary for a further pressure change, and which is therefore necessary to leave the operating point currently assumed as stationary (→ dynamic process). This is de facto nothing more, however, than the necessary compression volume flow to achieve the required pressure change according to the reference trajectory $\dot{p}_{set}$. In addition to the parameters to be determined operating point-dependently on the basis of the characteristic diagram K_S and T_S , only the setpoint value change $\dot{p}_{set}$ is necessary, which directly follows from the reference trajectory p_{set}, provided this is differentiable at least once, i.e. a pressure ramp is predefined as setpoint profile. The maximum achievable rate of rise of the pressure ramp is naturally once again dependent on the actuator dynamics. A further improved control behavior can be achieved through this additional operating point-dependent model-based precontrol term, as the actuating signal component necessary to realize the compression volume flows no longer has to be generated via the feedback controller and thus the control error.

5 Summary and conclusion

In principle, very good control results can be achieved using the stationary characteristic diagram in a 2DOF structure as model-based feedforward control. A method has been presented, which allows the drive characteristic diagram existing in reality to be reliably identified using just a few measured data. This method is essentially based on radial basis function networks, a special class of artificial neural networks. Using this method, the effort involved in characteristic diagram identification can be reduced to around 10% of the original value, and equivalent or even better control results can be expected than originally. In addition, a method also based on the drive characteristic diagram was demonstrated, which enables the feedback control parameters to be adapted operating point dependently. Both methods can in principle be implemented as real time-capable algorithms. The entire 2DOF control design can therefore be considered as a coherent and logical overall concept, which is based on the knowledge of a sufficiently accurate stationary model in the form of a nonparameteric look-up table. Both methods were described using the concrete example of an industrial deep drawing press. These are not limited to this specific drive system in principle, however, but can also be transferred to other drive systems. The characteristic diagram optimization in particular is a universally valid systematic concept which can be applied to any drive system, provided appropriate sensors are available for measuring stationary system states.

Nomenclature

Variable	*Description*	*Unit*
A	Area	[m²]
C_H	Hydraulic Capacity	[m³/Pa]
d	RBF Distance	-
e	Control/Model Error	-
E_{Fl}	Bulk Modulus Fluid	[Pa]
k_V	Valve Coefficient	[lpm/V·bar$^{0.5}$]
K	Gain Factor	-
l	Length	[m]
p	Pressure	[bar]
u	Control Signal/Voltage	[V]
T	Time Constant	[s]
V	Volume	[m³]
Q	Volume Flow	[m³/s]
x	Position	[m]
$\dot{x}$	Velocity	[m/s]
CD	Characteristic Diagram (Look-Up Table)	-
OP	Operating Point	-
x	Input Space	-
σ	RBF Form Parameter	-
ψ	Base Function	-

References

/1/ Horowitz I. M.; *Synthesis of Feedback Systems*, Academic Press, 1963

/2/ Räcklebe S., Radermacher T., Weber J., *Reduction of cycle time for injection moulding machines with electric hydrostatic drives*. In: 12th Scandinavian International Conference on Fluid Power, Tampere, Finland, May 18-20, 2011

/3/ Helmke M., Majer, H., Thanassakis, A., *Improvement of hydraulic control quality for deep drawing presses through retrofit*. In: 10th International Fluid Power Conference, 10. IFK, Dresden, Germany, pp 367–378, March 8-10, 2016

/4/ Heiss M., *Kennfelder in der Regelungstechnik*. In: at – Automatisierungstechnik, Volume 43, No. 8, pp 363-367, 1995, DOI: 10.1524/auto.1995.43.8.363

/5/ Isermann, R., Münchhof, M., *Identification of dynamic systems: An introduction with applications*, Springer, Heidelberg New York, 2011. ISBN: 3540788786

/6/ Müller Weingarten AG, *Produktportfolio*, Müller Weingarten AG, Weingarten, Germany, 2005

/7/ Moog GmbH, *Datenblatt Proportionalventile Baureihe D660*, Moog GmbH, Böblingen, 2005

/8/ Kroll, A., *Computational Intelligence: Eine Einführung in Probleme, Methoden und technischen Anwendungen,* München Oldenbourg, 2013, ISBN: 3486737422

/9/ Lunze, J., *Regelungstechnik 1: Systemtheoretische Grundlagen, Analyse und Entwurf einschleifiger Regelungen*, 10th edition, Springer, Berlin Heidelberg, 2014, ISBN: 978-364-25390-9-1